



RESEARCH ARTICLE / ARAŞTIRMA MAKALESİ

## Parametric Design of Torsional Springs Based on Fatigue Life

### Burulma Yaylarının Yorulma Ömrü Tabanlı Parametrik Tasarımı

Şafak Engin <sup>1</sup>, Binnur Gören Kırıl <sup>2\*</sup>

<sup>1</sup> Dokuz Eylül University, The Graduate School of Natural and Applied Sciences, Department of Mechanical Engineering, İzmir, TÜRKİYE

<sup>2</sup> Dokuz Eylül University, Faculty of Engineering, Department of Mechanical Engineering, İzmir, TÜRKİYE

Corresponding Author / Sorumlu Yazar\*: binnur.goren@deu.edu.tr

#### Abstract

Torsion springs are used extensively in numerous industrial applications, including robotic systems, toys, latches, door hinges, clock mechanisms, and vibration isolation systems. Design characteristics of these springs have a big impact on both the mechanical behavior of the spring and the system it's installed in. The purpose of this work is to examine how the geometries of parametrically modeled springs affect their mechanical properties using the finite element method. Furthermore, the effect of spring geometry variations on component fatigue life has also been examined in a specific fixed packaging scenario because springs frequently need to be crammed into quite small packages. The findings of this research will offer a new viewpoint on torsion spring design and optimization. It is meant to contribute to the relevant sector and literature through the procedure stages of three-dimensional geometric modeling for torsion spring design with CREO PARAMETRIC software and the results of structural and fatigue analysis obtained with ANSYS WORKBENCH software.

**Keywords:** Torsion spring, Parametric modeling, Parametric formulation, Finite element analysis

#### Öz

Robotik sistemler, oyuncaklar, mandallar, kapı menteşeleri, saat mekanizmaları ve titreşim izolasyon sistemleri dahil olmak üzere çok sayıda endüstriyel uygulamada büyük ölçüde burulma yayları kullanılmaktadır. Bu yayların tasarım özelliklerinin hem yayın mekanik davranışı hem de kurulduğu sistem üzerinde büyük etkisi bulunmaktadır. Bu çalışmanın amacı, parametrik olarak modellenen yayların geometrilerinin mekanik özelliklerini nasıl etkilediğini sonlu elemanlar yöntemi kullanarak incelemektir. Ayrıca, yayların sıklıkla oldukça küçük paketlere sıkıştırılması gerektiği için yay geometrisi değişimlerinin bileşen yorulma ömrü üzerindeki etkisi belirli bir sabit paketleme senaryosunda incelenmiştir. Bu çalışmanın sonuçları, burulma yaylarının tasarımı ve optimize edilmesi için yeni bir perspektif sunacaktır. Burulma yayı tasarımına yönelik CREO PARAMETRIC yazılımı ile üç boyutlu geometrik modellemenin işlem aşamalarının ve ANSYS WORKBENCH yazılımı ile elde edilen yapısal ve yorulma analiz sonuçlarının ilgili sektöre ve literatüre katkı sağlaması amaçlanmaktadır.

**Anahtar Kelimeler:** Burulma yayı, Parametrik modelleme, Parametrik formülizasyon, Sonlu elemanlar analizi

#### 1. Introduction

Mass production, which is a cause and also a result of today's developing technology and industry, is pushing its limits day by day in order to provide faster responses and products. This limit has shown itself day by day in the areas of design, verification and prototypes per unit, as well as the production time per unit. While mass production is important, serial design and verification are also important. In fact, a time-consuming design, verification and prototyping study may end before the mass production phase.

Reducing energy waste and making sustainability and environmentally friendly processes more widespread are among the main goals of manufacturing facilities [1]. For this reason, it is very important that design processes, just like production processes, are combined with software supports and can provide fast results. Just as a fast and high-precision product output can be obtained thanks to a process in mass production, a fast and high-precision model output should be obtained by following the same logic in design.

In this regard, the springs used both in the finished product and in the machines or fixtures that produce this product are important machine elements that have a difficult design and may require more than one prototype during the design phase.

A spring is a flexible element that stores energy and is used to apply force or torque. The force can be linear compression/tensile or radial. If it is necessary to give an example of torque under the heading of radial force, closing a refrigerator door or the mechanism of door handles used at home can be considered. Springs naturally store energy when force is applied and return to their previous positions when the applied force is removed [2].

Mechanical engineering is becoming a growing field with an increased level of automation and smart manufacturing processes. This leads to a higher parameter control, i.e. reduction of product defects, reduction of unplanned downtime and improved flexibility. Like other mechanical components, spring design is done with various tables and charts containing predetermined specifications. The exact specification of the

spring amount is still not fully known to a certain extent. Despite spring theory and accumulated practical knowledge, the variety of materials, sizes and shapes is so wide that the design process represents a serious engineering challenge. Even with computer assistance, designers often need to simplify the spring design procedure [3].

Although current computer-aided design technology is very efficient, especially for graphical presentations, it is insufficient to provide support to the designer. Synthesis has the greatest impact on production cost and product quality. Therefore, automating synthesis can improve the efficiency and quality of the design process. By applying object-oriented programming techniques, a suitable support system architecture can be created for underdeveloped areas of the design process [3].

**2. Material and Method**

In this study, Creo Parametric software was used for modeling and certain boundary conditions were taken into account in modeling. The most important of these conditions are the height and width of the place where the torsion spring will be used and the nominal position torque that the spring must provide. In order to determine how effective which parameter is, nine different torsion springs with the same package volume and capable of providing the same torque were modeled. Figure 1 shows images of an example spring in its unstretched position and the same spring in its nominal position.

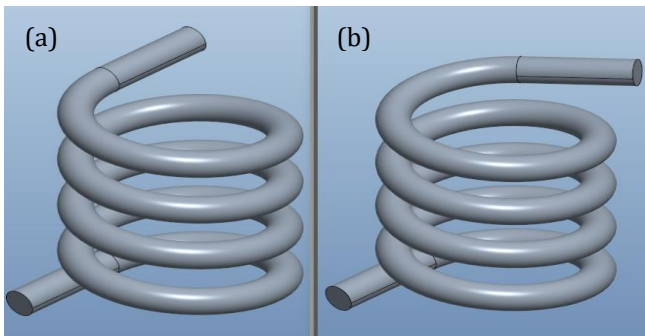


**Figure 1.** Torsion spring in (a) unstretched position (b) nominal position.

The outer length of the springs is 52 mm, their outer diameter is 30 mm and the torque they provide in the nominal position is 17 N.m. The variables will be the number of windings and wire diameter. Table 1 lists the basic features of the springs examined.

**Table 1.** Fundamental parameters of modeled torsion springs.

Nr	Torque (N.m)	Number of windings	Wire diameter (mm)	Nominal position angle (°)
1	17	4	6	33.5
2	17	4	7	17.6
3	17	4	8	10.0
4	17	4	9	6.0
5	17	5	6	41.9
6	17	5	7	21.9
7	17	5	8	12.5
8	17	6	6	50.3
9	17	6	7	26.3

**2.1. Material**

Structural and fatigue analysis of the springs modeled within the scope of the study was carried out. Figure 2 shows the comparison of oil tempered DIN EN 10270-2:2012 standard materials used as spring materials. This figure also includes the relationship between fatigue strength and tensile strength [4,5].

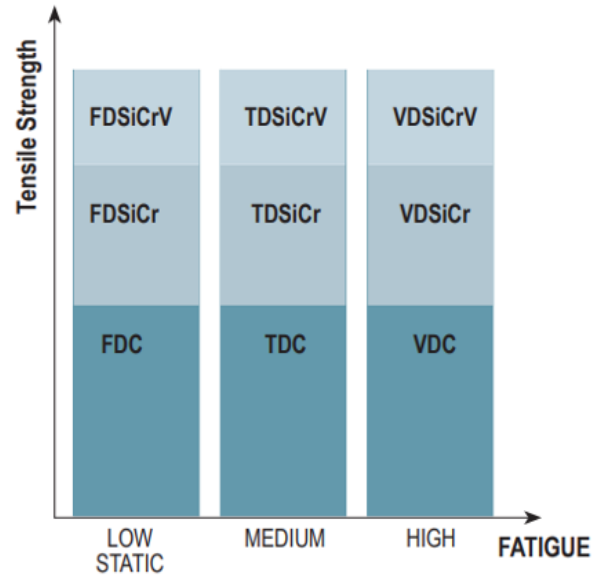


**Figure 2.** Tensile strength of oil tempered spring steels with respect to fatigue [4, 5].

In the structural and fatigue analyzes in this study, VDSiCr material was used because the requirement for high fatigue strength was taken into account. According to DIN EN 10270-2:2012 standard, tensile strength tends to decrease as the wire diameter used increases. Table 2 shows tensile strengths varying according to wire diameter.

The wire thickness of the springs to be examined was determined as 6 mm, 7 mm, 8 mm and 9 mm. ANSYS Workbench software was used in the analysis and the tensile strength was taken into account as 1700 MPa.

**Table 2.** Tensile strength according to wire diameter.

Nominal diameter (a < Ø ≤ b) [mm]	Diameter tolerance (±) [mm]	Tensile Strength [N/mm <sup>2</sup> ]
5.60 - 6.00	0.040	1760 - 1860
6.00 - 6.50	0.040	1760 - 1860
6.50 - 7.00	0.040	1710 - 1810
7.00 - 8,00	0.045	1710 - 1810
8.00 - 9.00	0.045	1670 - 1770

**2.2. Structural Analyses**

At this stage of the study, structural analyzes of nine different models that would fit into the same package and provide the same torque were first carried out using the finite element method. With these analyses, torque was applied to the springs and the springs were brought to their nominal position. Thus, the

amount of twisting obtained after applying the torque and the stresses occurring in the spring depending on the wire diameter were examined. The purpose of the analysis is to examine the mechanical behavior of the wire that is wound and twisted to obtain torque. In addition, since the leg of the spring are ineffective in applying torque, the leg parts of the springs were not included in the analysis. While modeling the specimens, the package size was fixed, and the number of windings and wire diameters of the springs were determined as variable. In order to investigate the effect of the variables on the result, the effect of the wire diameter on the results will be questioned by applying a 17 N·m torque to the specimens, and the effect of the number of windings on the fatigue strength will be observed by applying an additional twist angle of 10° to the nominal position values obtained by applying 17 N·m torque on all specimens.

**2.2.1. Finite element model**

While creating the mesh, the studies in the literature were taken into consideration, and the torsion springs solution mesh was realized using the sweep method as shown in Figure 3.



**Figure 3.** Finite element model of torsion spring [6].

**2.2.2. Boundary conditions**

Regarding the sensitivity of the results, it is crucial to accurately identify the boundary conditions that must be applied to the finite element models of torsion springs whose geometries have been determined. Two-step boundary conditions were established and two distinct torque values were used to the spring finite element models. In every instance, torque was given to one end of the models while the other was fixed. For the first and second phases, the initial applied torque value was found to be 17 N·m. This initial torque application is meant to move the models from their unstretched position to their nominal position. Figure 4 displays the initial applied torque and its stages.

The second torque applied is in two steps; in the first step, 0 N·m torque is applied, and in the second step, different torque values are applied to each spring. Since the spring rate values of the models are different, different torque values are expected for different spring types. In this study, by applying different torque values, an additional twist angle of 10° was applied to the nominal position. The new position obtained with the additional twist angle can be called the maximum position. The second applied torque and its steps are shown in Figure 5.

The spring rate and maximum position torque values of the models are shown in Table 3.



**Figure 4.** Initial torque applied and its steps.



**Figure 5.** Second torque applied and its steps.

**Table 3.** Spring rate and maximum position torque values of the models.

Nr	Spring rate (Nm/°)	Maximum Position Torque (N·m)
1	0.51	19.54
2	0.97	21.84
3	1.70	25.52
4	2.82	31.09
5	0.41	19.03
6	0.77	20.87
7	1.36	23.81
8	0.34	18.69
9	0.65	20.23

**2.3. Fatigue analyses**

To generate a logarithmic graph incorporating the fatigue test data, the Excel application was utilized to tabulate each number. Table 4 has two columns dedicated to stress. The values acquired by utilizing the logarithmic equation determined by regression on the graph and entered into the ANSYS Workbench application are the stress values in the third column, whereas the values in

the first column contain the values taken in Figure 6. In Figure 6, the regression curve is displayed.

**Table 4.** Stress, cycle and calculated stress values.

Stress (MPa)	Cycle	Calculated stress (MPa)
670	2·10 <sup>5</sup>	642.78
660	4·10 <sup>5</sup>	636.66
650	5·10 <sup>5</sup>	634.70
620	6·10 <sup>5</sup>	633.86
610	8·10 <sup>5</sup>	630.55
610	1·10 <sup>6</sup>	628.58
600	2·10 <sup>6</sup>	625.01
620	2·10 <sup>6</sup>	622.92
600	7·10 <sup>7</sup>	591.12
570	2·10 <sup>8</sup>	581.86
550	8·10 <sup>8</sup>	569.64
570	1·10 <sup>9</sup>	567.67
600	1·10 <sup>9</sup>	566.06
580	2·10 <sup>9</sup>	562.49
570	4·10 <sup>9</sup>	555.90
590	5·10 <sup>9</sup>	553.84
530	5·10 <sup>9</sup>	553.48
520	6·10 <sup>9</sup>	551.87
560	7·10 <sup>9</sup>	551.17
560	7·10 <sup>9</sup>	550.51
520	8·10 <sup>9</sup>	549.34

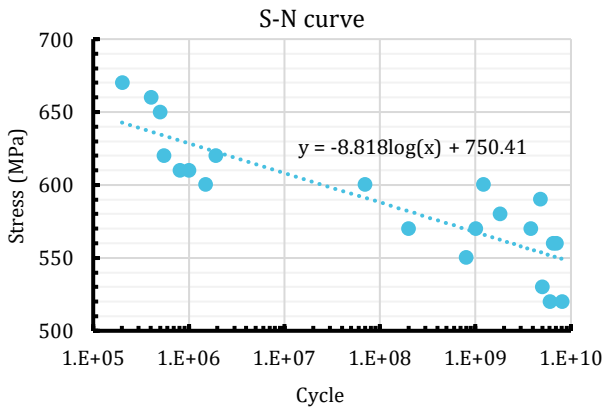


**Figure 6.** Stress-cycle graph used for regression.

**3. Results**

**3.1. Structural analysis**

In the structural analysis performed, four different results were obtained for each model. These are as follows, respectively:

- Maximum displacement from unstretched position to nominal position (a),
- Maximum stress from unstretched position to nominal position (b),
- Maximum displacement from unstretched position to maximum position (c),

- Maximum stress (d) from unstretched position to maximum position.

Figure 7-15 shows the variation of these four values on the spring for nine different specimens.

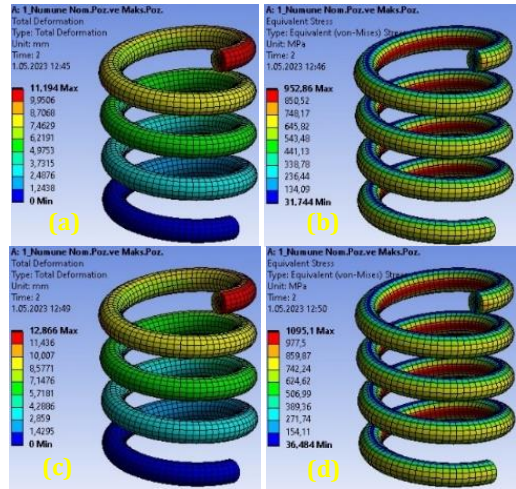


**Figure 7.** Result of structural analysis for specimen 1.

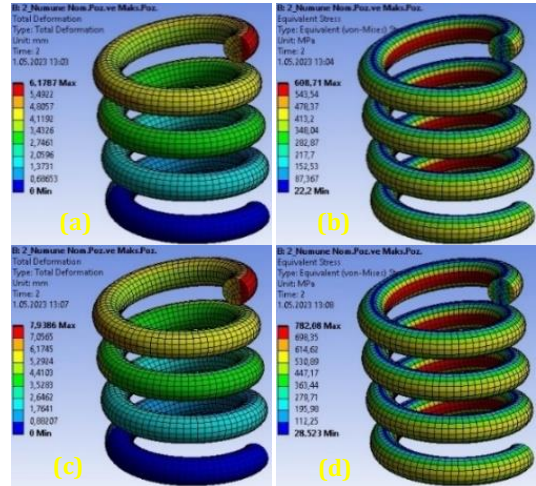


**Figure 8.** Result of structural analysis for specimen 2.

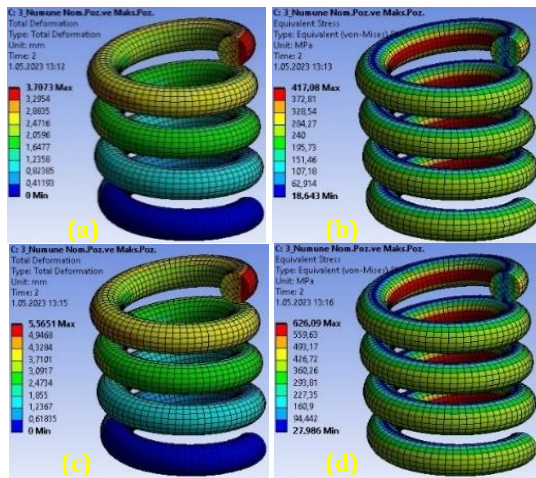


**Figure 9.** Result of structural analysis for specimen 3.

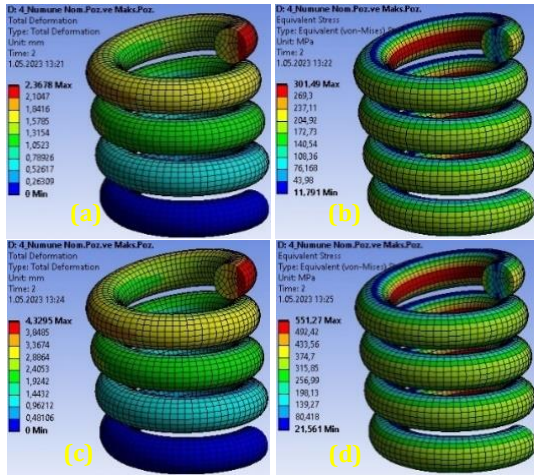


Figure 10. Result of structural analysis for specimen 4.

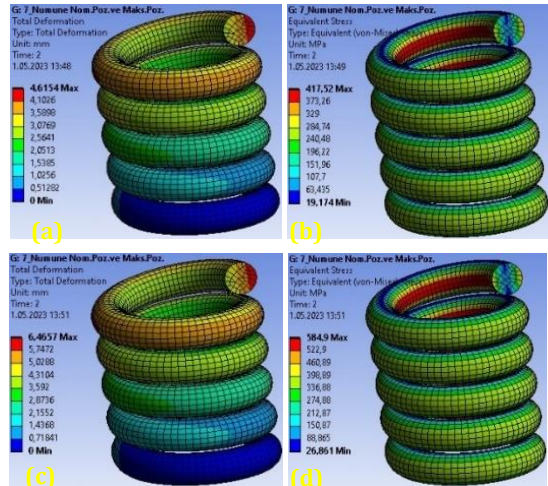


Figure 13. Result of structural analysis for specimen 7.

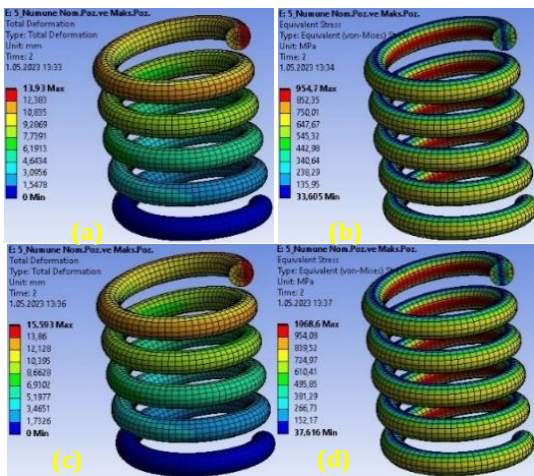


Figure 11. Result of structural analysis for specimen 5.

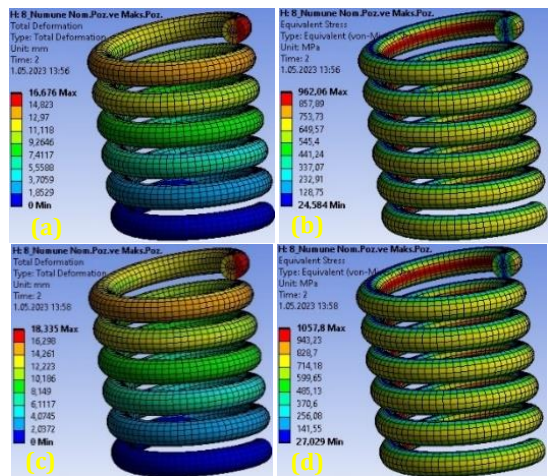


Figure 14. Result of structural analysis for specimen 8.

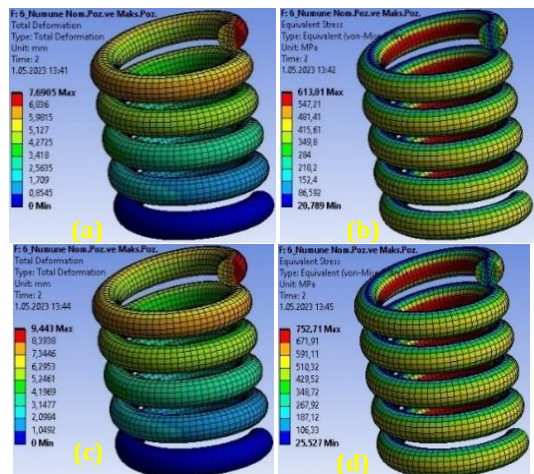


Figure 12. Result of structural analysis for specimen 6.

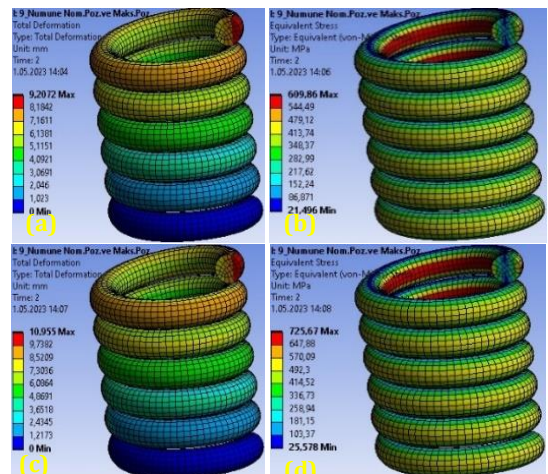


Figure 15. Result of structural analysis for specimen 9.

### 3.2. Fatigue analysis

In the structural analysis performed, four different results were obtained for each specimen. These are as follows, respectively:

- Fatigue life from unstretched position to nominal position (a),
- Fatigue safety from unstretched position to nominal position (b),
- Fatigue life from unstretched position to maximum position (c),
- Fatigue safety from unstretched position to maximum position is (d).

Figure 6-24 shows the variation of these four values over the spring for nine different specimens.

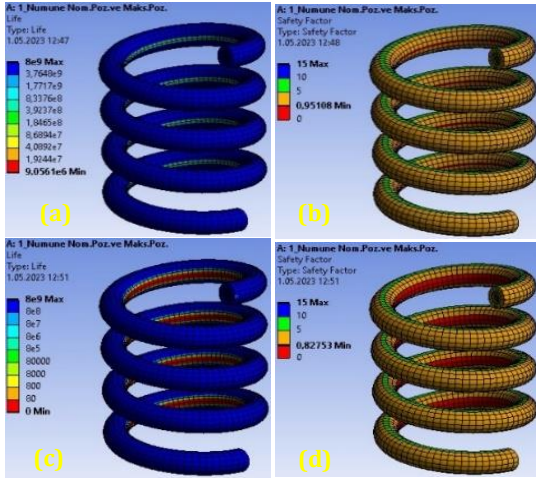


Figure 16. Results of fatigue analysis for specimen 1.

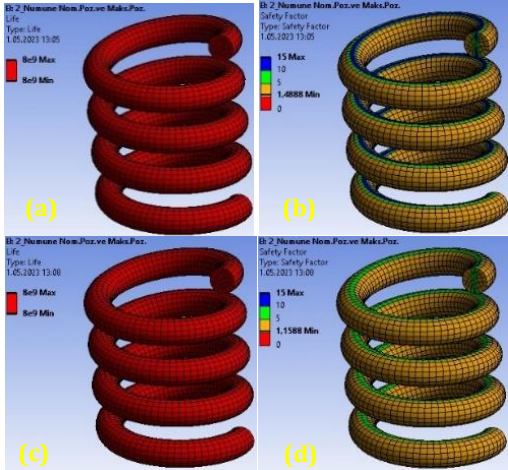


Figure 17. Results of fatigue analysis for specimen 2.

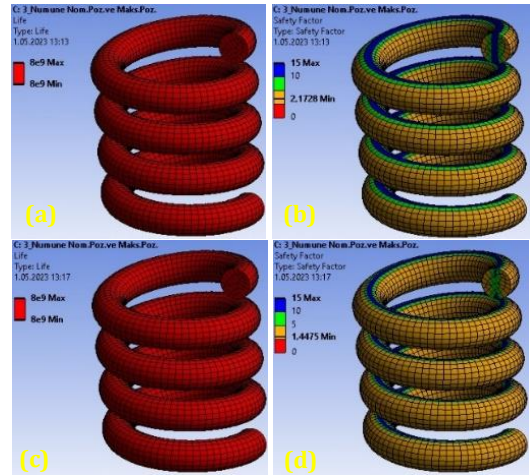


Figure 18. Results of fatigue analysis for specimen 3.

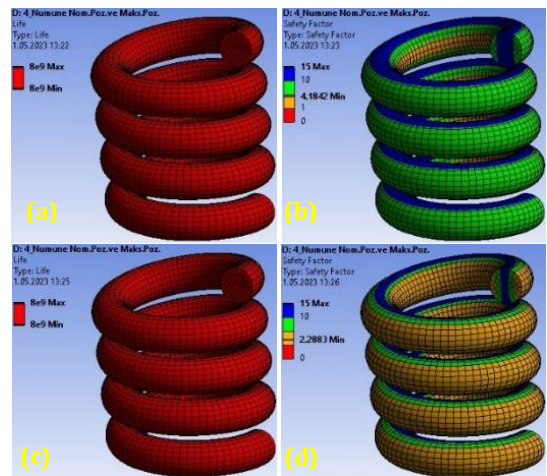


Figure 19. Results of fatigue analysis for specimen 4.

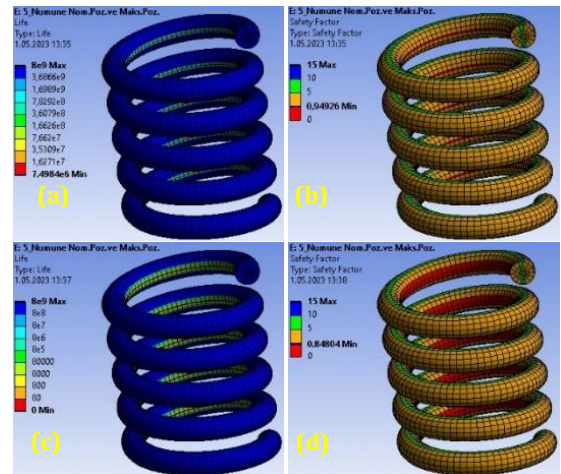


Figure 20. Results of fatigue analysis for specimen 5.

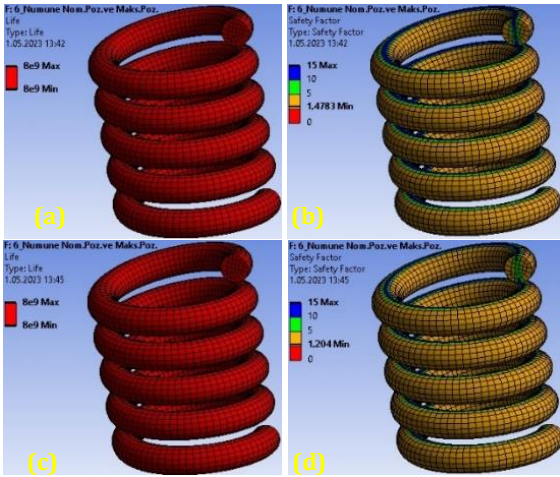


Figure 21. Results of fatigue analysis for specimen 6.

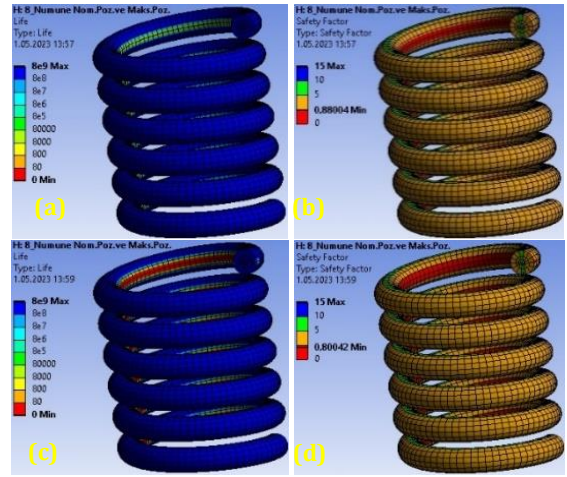


Figure 23. Results of fatigue analysis for specimen 8.

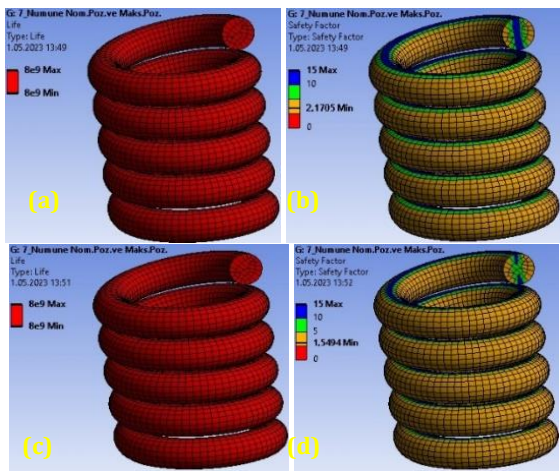


Figure 22. Results of fatigue analysis for specimen 7.

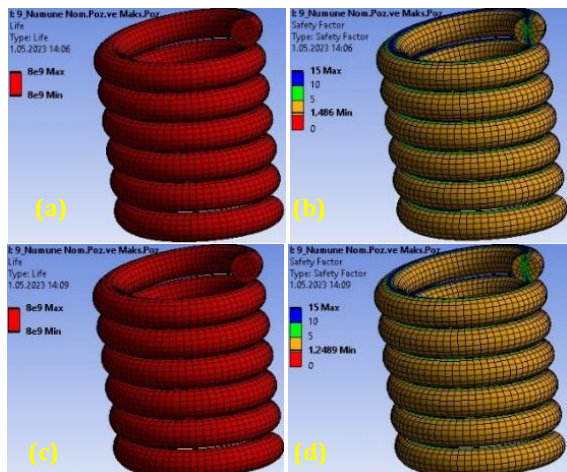


Figure 24. Results of fatigue analysis for specimen 9.

Table 5. Numerical results of structural analyses.

Nr	Unstretched position		Nominal position			Maximum position		
	Number of windings	Diameter of wire (mm)	Max. Stress (MPa)	Number of fatigue cycle	Fatigue Safety Factor	Max. Stress (MPa)	Number of fatigue cycle	Fatigue Safety factor
1	4	6	952.86	$9.056 \cdot 10^6$	0.951	1095.1	0	0.828
2	4	7	608.71	$8 \cdot 10^9$	1.489	782.08	$8 \cdot 10^9$	1.159
3	4	8	417.08	$8 \cdot 10^9$	2.172	626.09	$8 \cdot 10^9$	1.448
4	4	9	301.49	$8 \cdot 10^9$	4.184	551.27	$8 \cdot 10^9$	2.288
5	5	6	954.7	$7.498 \cdot 10^6$	0.949	1068.6	0	0.848
6	5	7	613.01	$8 \cdot 10^9$	1.478	752.71	$8 \cdot 10^9$	1.204
7	5	8	417.52	$8 \cdot 10^9$	2.171	584.9	$8 \cdot 10^9$	1.549
8	6	6	962.06	0	0.880	1057.8	0	0.800
9	6	7	609.86	$8 \cdot 10^9$	1.486	725.67	$8 \cdot 10^9$	1.249

The evaluations will look at the impact of changing the number of turns on the maximum stress and fatigue safety factor by maintaining a constant wire diameter. Similarly, the impact of altering the wire diameter on the fatigue safety factor and maximum tension will be investigated while maintaining an unchanged number of windings.

**3.3. Maximum von Mises Stress with respect to Windings Number**

In this section, the effect of the number of windings on the maximum von Mises stress for a certain wire diameter was investigated. Figures 25, 26 and 27 shows the maximum von Mises stress changes depending on the number of windings for 6 mm, 7 mm and 8 mm of wire diameter, respectively.

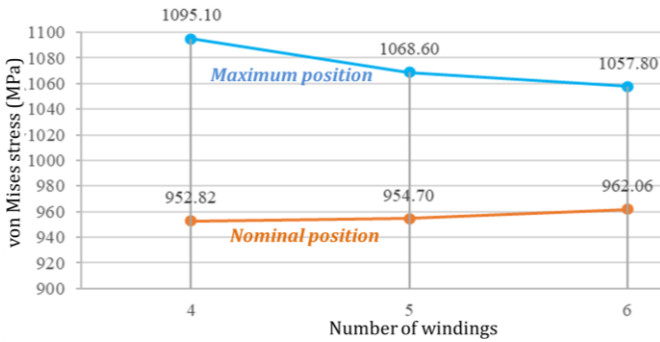


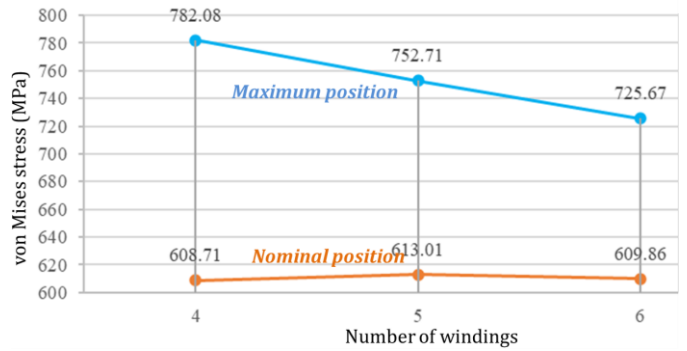
**Figure 25.** Variation of the maximum stress depending on the number of windings for 6 mm wire diameter.

These graphs show the stresses obtained in both the nominal position and the maximum position. As can be seen in Figure 25, when the springs are in the nominal position, that is, when all the springs are in a position to produce 17 N.m torque, there is a slight increase in tension depending on the number of windings. In fact, cross-sectional areas should yield the same stress results if the same material is utilized. However, in this example, the maximum tension tends to increase as the number of windings increases since the spring rate decreases. Because the spring needs to be spun more to achieve the same torque value when the spring rate declines. The maximum stress, which tends to grow, is explained by the rising displacement that occurs per unit volume.

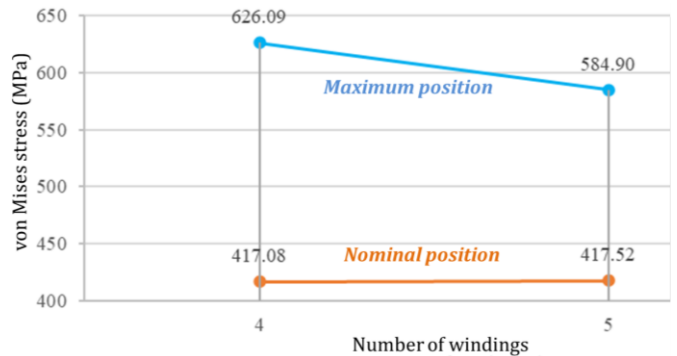
If comparison is made for the maximum position, the reason for the decreasing stress tendency with equal torsion applied to the springs brought to the nominal position is again related to the spring rate. Because the spring rate, which tends to decrease with the increasing number of windings, will provide a gradually lower torque at the same amount of rotation. Naturally, the increase in the number of windings in the models tends to increase in the nominal position, while it shows a decreasing trend in the maximum position.

Figure 26 is a comparison made for 7 mm wire diameter, and when the tension value at the maximum position is examined, it is seen that there is a similar trend to Figure 25. On the other hand, it was observed that there was no significant change in the maximum stress values in the nominal position.

Similar trends can be seen in Figure 27. However, in this figure it is more clearly seen that these trends in the nominal position the maximum stress values gradually decrease with the increase in wire diameter. The reason for this can be interpreted as the effect of the increase in wire ratio as the wire diameter increases.



**Figure 26.** Variation of maximum stress depending on the number of windings for 7 mm wire diameter.



**Figure 27.** Variation of maximum stress depending on the number of windings for 8 mm wire diameter.

**3.4. Maximum von Mises Stress with respect to Wire Diameter**

In this section, the effect of the diameter of the spring wire on the maximum von Mises stress for a certain winding number was investigated. Figures 28, 29 and 30 shows the maximum von Mises stress changes depending on the number of windings for 4, 5 and 6 of winding number, respectively. These graphs show variation of the maximum stress values for both the nominal position and the maximum position.

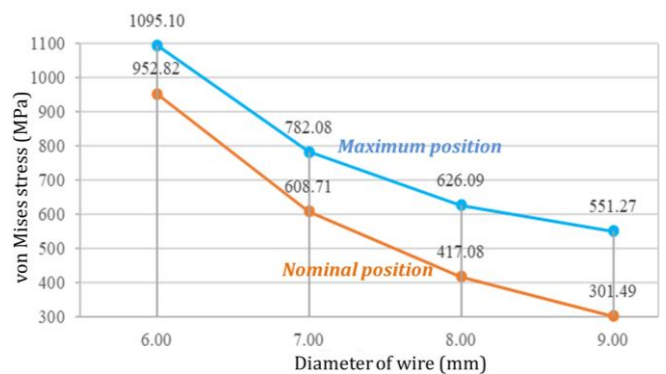


**Figure 28.** Variation of maximum stress depending on the wire diameter for four windings.

As seen from Figure 28, in the nominal position, in other words, when all springs are in a position to produce 17 N.m torque, it is seen that the maximum stress value decreases depending on the wire diameter. This is related to the increasing spring rate as the cross-sectional area increases. While the required torque is constant, the displacement caused by the constant force applied to the spring will decrease due to the increasing wire diameter as

the spring rate increases. Thus, the maximum stress value will decrease due to the lower displacement (torsion angle).

When comparing the maximum position to the nominal position, it can be observed that the maximum stress tends to diminish less with an equal torsion angle applied to the springs brought to the nominal position. Once more, the spring rate determines this. Because the torque produced at the same amount of rotation will grow with the spring rate, which tends to increase with increasing wire diameter. Increasing torque will, of course, cause the maximum stress to reduce less than the nominal position will decrease.

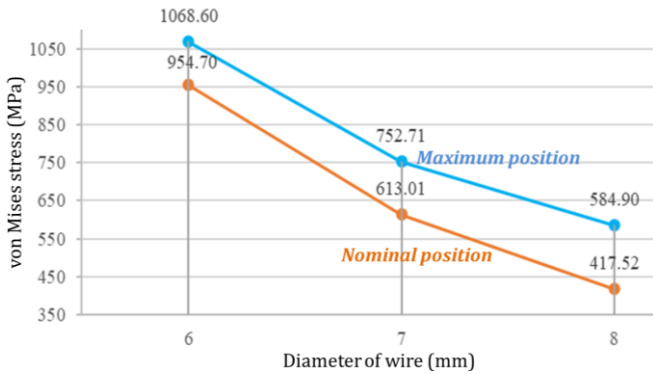


**Figure 29.** Variation of maximum stress depending on the wire diameter for five windings.

Figures 28 and 29 depict a similar pattern and were created for the model with five windings. The maximum stress in the maximum position tends to diminish comparatively less than the nominal position, whereas the maximum stress in the nominal position tends to decline progressively.

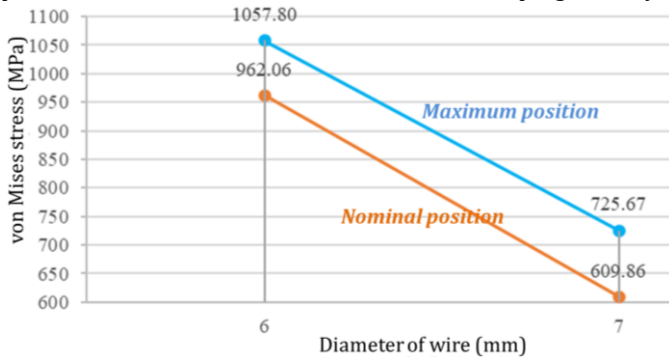


**Figure 30.** Variation of maximum stress depending on the wire diameter for six windings.

The same patterns become evident when considering Figure 30, which shows that the stress value produced in the nominal position the maximum stress value decreases more with increasing wire diameter than the maximum position decreases.

**3.5. Fatigue Safety Factor with respect to Windings Number**

First, the fatigue safety factor of the specimens with varying winding number based on a specific wire diameter was compared. It can be assumed that the spring can theoretically operate under dynamic loading under defined conditions with an infinite number of cycles if the safety factor obtained in the comparisons is 1 or above. It can be easily emphasized that a spring shape is unsuitable for dynamic operation if the safety factor is less than 1. Figures 31, 32 and 33 show the fatigue safety factor changes depending on the number of windings for 6 mm, 7 mm and 8 mm of wire diameter, respectively. These graphs show

the fatigue safety factors obtained in both the nominal position and the maximum position.

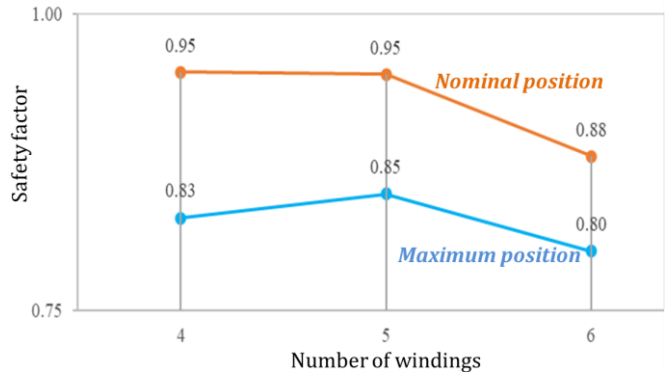


**Figure 31.** Variation of safety factor depending on the winding number for 6 mm of wire.

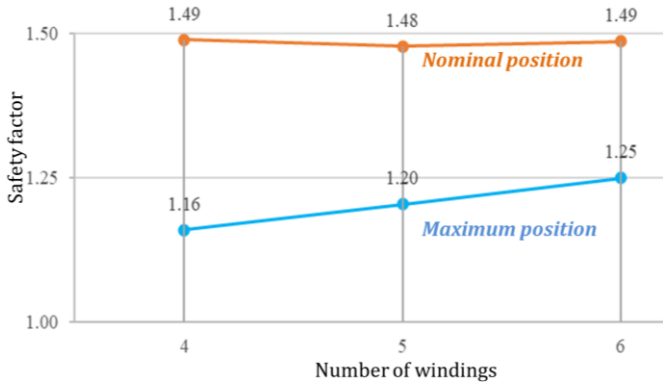
Figure 31 illustrates that the spring intended for the package scenario that was previously estimated has a wire diameter of 6 mm, which is not acceptable for dynamic operation due to safety factors below 1. Based on the computations conducted and the number of cycles listed in Table 5, it was predicted that there would be  $9.056 \times 10^6$  cycles when there were four windings,  $7.498 \times 10^6$  cycles when there were five windings, and 0 cycles when there were six windings. The number of cycles to be employed must be determined when selecting and designing for locations with a fatigue safety factor less than 1, as the  $8 \times 10^6$  cycle count is recognized as an unlimited life.

In the nominal position in the specified chart; In other words, when all the springs are in a position to produce 17 N-m of torque, it can be interpreted that the safety factor remain close to a constant line despite the increase in the number of windings. In the maximum position, it can be evaluated that the safety factor increases with the increasing number of windings. However, it should be considered that the decrease in the fatigue safety factor in both the nominal position and the maximum position, seen when the number of windings is 6, may be related to the solution network coming from the analysis program and made. To better understand and interpret this, other graphs should also be evaluated.

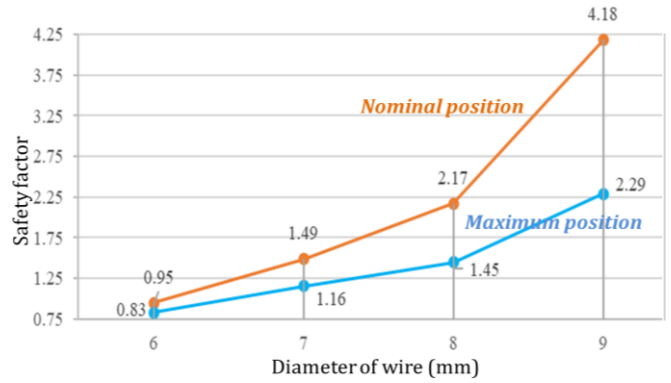
It is anticipated to see an increase based on the number of windings at the maximum position, as the spring rate will decrease with an increase in winding count. For springs with a large number of windings, less torque will be applied because the torsion angle applied to all models remains constant beyond the nominal position. This validates the upward trend.

In contrast to Figure 31, Figure 32 shows that the 7 mm wire diameter chosen for the package scenario that was first decided upon is appropriate for dynamic operation because the safety factor is greater than 1.

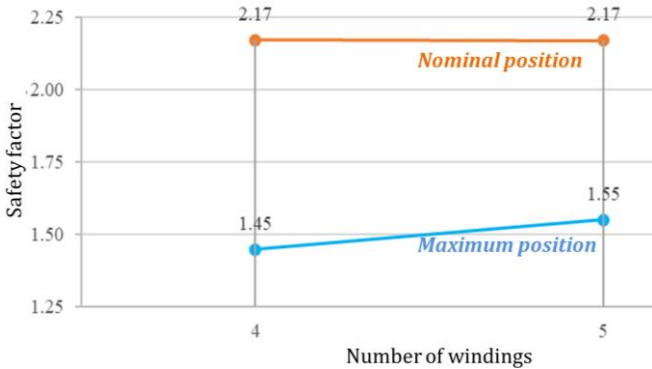
According to the above figure, even with more windings, the safety factor will still be quite close to a constant line when the springs are all in a position to produce 17 N-m of torque, or in the nominal position. An increasing safety factor is shown at the maximum position as the number of windings increases. The angle between the applied nominal position and the maximum position will cause the spring to produce less torque as the spring rate decreases. As a result, the safety factor will probably rise.



**Figure 32.** Variation of safety factor depending on the winding number for 7 mm .



**Figure 34.** Variation of safety factor depending on the wire diameter for four windings.



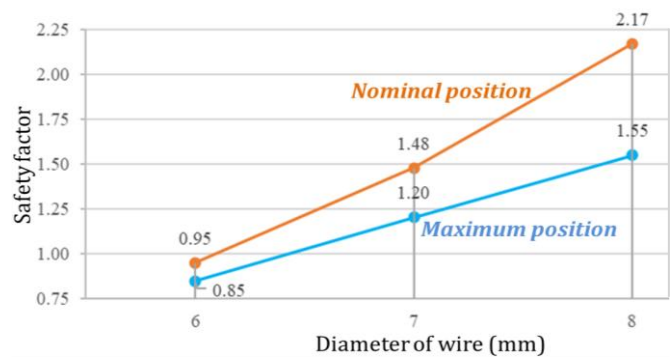
**Figure 33.** Variation of safety factor depending on the winding number for 8 mm

Figure 33 shows that the specimens having parameters in this figure are appropriate for a dynamic loading. Similarly, as the number of windings increases, the fatigue safety factor in the maximum position rises in proportion, whereas the fatigue safety factor in the nominal position remains constant. Another factor at play here is that the fatigue safety factor increases at the maximum location in step with the increasing wire diameter. The anticipated increase in spring strength with increased wire diameter helps to explain this.

**3.6. Fatigue Safety Factor with respect to Wire Diameter**

In this section, the effect of the diameter of the spring wire on the fatigue safety factor for a certain winding number was investigated. Figures 34, 35 and 36 shows the change in the fatigue safety factor depending on the wire diameter for four, five and six of winding number, respectively. These graphs include variation of the fatigue safety factor values for both the nominal position and the maximum position.

As can be seen in Figure 34, the fatigue safety factor increases with the increasing wire diameter in the nominal and maximum positions. It is an expected result that the stress values decrease as the cross-sectional area of the wire increases. Additionally, the chart demonstrates that upward tendency in the nominal position is greater than the maximum position's. This is caused by the fact that the torque given to the bigger wire diameter is greater, the additional twisting angle applied after the nominal position, and the increasing spring rate applied in tandem with the increasing wire diameter. As a result, the maximum position has a lower fatigue safety factor increase than the nominal position.



**Figure 35.** Variation of safety factor depending on the wire diameter for five windings

In Figure 35, the safety factor in the nominal position and maximum position increases in parallel with the increasing wire diameter. As in the previous graph, tension values decrease as the wire diameter increases. Similarly, the upward trend in the nominal position is higher than in the maximum position. This is again due to the torsion angle difference between the nominal position and the maximum position, depending on the increasing wire diameter and increasing spring rate.

Figure 36 illustrates that the safety factor increases nearly parallel to each other at both the nominal and maximum positions as the wire diameter gets larger. As with the earlier graphs, it is anticipated that the structure will get stiffer as the cross-sectional area grows. On the other hand, as the number of windings increases, so does the increase in the fatigue safety factor brought about by the increased wire diameter. For instance, when the number of windings increases, the fatigue safety factor difference between 6 mm and 7 mm wire diameters progressively rises.

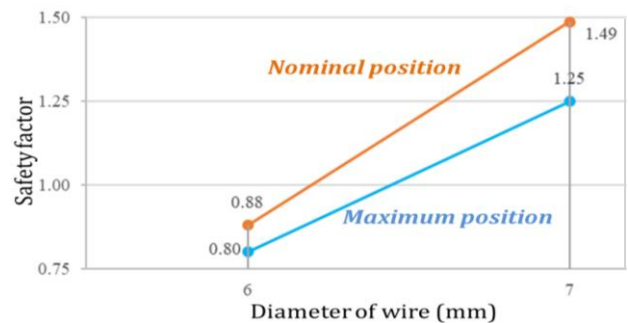


**Figure 36.** Variation of safety factor depending on the wire diameter for six windings

### 3. Conclusion

Within the scope of this study, the parametric design and structural analysis of torsion springs, one of the machine elements used for elastic energy accumulation, were carried out. First, the design boundary conditions were determined and a common package scenario was developed for the springs to operate in. By establishing a common nominal position and common maximum position for the various modeled torsion springs, analysis boundary conditions were established. The analysis looked into how the results were affected by torsion springs and the inputs needed for parametric design.

In the examinations, there are formulas, forms, websites or package programs that can calculate torsion springs. However, none of these provide a model for the designer. Parametric torsion spring design Creo Parametric modeling software was used for certain variables limited to the package scenario. In addition, the formulas that need to be entered into the program are also provided with this study. It has been created in a format that can be used by all designers, both in industry and literature.

In addition to designing a parametric model, nine different torsion springs were determined and their models were created in this study. Within the scope of the study, the effects of wire diameter and number of turns were examined with the results obtained from structural analyzes performed using ANSYS Workbench software. Since the wire diameter and number of turns are directly related to the spring rate, the effects of wire diameter and number of turns have been observed in both torque-oriented and torsion angle-oriented analyses.

According to the analysis results, the increase in wire diameter increases the fatigue safety factor and reduces the maximum stress. The factors that limit the designer in increasing the wire diameter during design are package size and mass. Since the package size is limited, the number of turns in relation to the wire diameter is also of great importance. As a result of the analysis made with the number of windings, the maximum stress decreases relatively with the increase in the number of windings, while the fatigue life safety factor increases slightly. It can be easily seen that these changes are quite low compared to the wire diameter. Therefore, instead of increasing the number of windings when designing, increasing the wire diameter will produce a more reliable product. The spring rate increasing with the increase in wire diameter will bring large torque differences in the twisting angle change. Therefore, it is important to pay attention to this during design.

Although this study is only about torsion springs, all other springs or, if necessary, all other machine elements can be designed with the same formulation idea and rapid results can be obtained. In this way, the industry can become more competitive by minimizing time loss in the design process.

#### **Ethics committee approval and conflict of interest statement**

This article does not require ethics committee approval. This article has no conflicts of interest with any individual or institution.

#### **Author Contribution Statement**

All authors contributed equally to the conception, design, execution, and interpretation of the study, as well as the preparation and revision of the manuscript.

### References

- [1] Brundage, M. P., Chang, Q., Li, Y., Arinez, J., & Xiao, G., 2014. Sustainable manufacturing performance indicators for a serial production line. *IEEE Transactions on Automation Science and Engineering*, 13(2), pp.676-687.
- [2] Mott, R. L., 2018. *Machine Elements in Mechanical Design*. EMV & JW.
- [3] Saric, I., Muratovic, E., Muminovic, A., Muminovic, A. J., Colic, M., Delic, M., & Mesic, E., 2021. Integrated intelligent CAD system for interactive design, analysis, and prototyping of compression and torsion springs. *Applied Sciences*, 12(1), 353.
- [4] European Standards, 2012. Steel wire for mechanical springs - Part 2: Oil hardened and tempered spring steel wire—Requirements with guidance for use (DIN EN Standard No. 10270-2:2012). Available at: <https://www.en-standard.eu/din-en-10270-2-steel-wire-for-mechanical-springs-part-2-oil-hardened-and-tempered-spring-steel-wire/>.
- [5] Vinco, 2023. Oil Tempered Steel Wire. Available at: [https://www.vinco.es/en/wire/oil-tempered-steel/#caracteristicas\\_mecanicas](https://www.vinco.es/en/wire/oil-tempered-steel/#caracteristicas_mecanicas).
- [6] Li, H. Y., & Li, X. L., 2013. Finite element analysis of the cylindrical helical torsional spring. In: *Applied Mechanics and Materials Vol. 397*, pp. 633-636. Trans Tech Publications Ltd.